

Cite this: *RSC Sustainability*, 2023, 1, 326

# From waste to wearable: an alternative waste stream for unusable textiles turned into piezoelectric textiles†

JoAnna Milam-Guerrero,<sup>a</sup> Dong-Jun Kwon,<sup>b</sup> Yun Young Choi,<sup>a</sup> Faraj Al-badani,<sup>a</sup> Jizhou Jiang,<sup>a</sup> Jennifer Schaefer<sup>a</sup> and Nosang V. Myung<sup>a\*</sup>Received 5th October 2022  
Accepted 11th January 2023

DOI: 10.1039/d2su00068g

rsc.li/rscsus

In response to the growing fashion and textile industry, a market of reuse and recyclability to create alternative waste streams has emerged. With a more eco-friendly mindset, companies have begun to embrace clothing reuse through several means of recycling techniques (chemical, mechanical, thermal) or reuse; however, most spent clothing is disposed of. Herein, a novel method of recycling, for specific materials, is presented. From purchased secondhand clothing, made of either acrylic or nylon-6, an electronic textile is electrospun and implemented into a wearable smart mask demonstrating the feasibility with which textile waste can be transformed into a high performance energy generating and/or sensing material.

## Sustainability spotlight

In response to the growing fashion and textile industry, a market of reuse and recyclability to create alternative waste streams has emerged. With a more eco-friendly mindset, companies have begun to embrace clothing reuse through several means of recycling techniques (chemical, mechanical, thermal) or reuse; however, most spent clothing is disposed. Herein, a novel method of recycling, for specific materials, is presented. From purchased secondhand clothing, made of either acrylic or nylon-6, an electronic textile is electrospun and implemented into a wearable smart mask demonstrating the feasibility with which textile waste can be transformed into a high performance energy generating and/or sensing material.

## Introduction

Researchers and scientists are continually seeking new ways to achieve carbon neutrality for a more sustainable society and overall healthier future.<sup>1–5</sup> Some often historically overlooked areas, such as the fashion and the textile industries, make a surprisingly large anthropogenic environmental impact. The term most often used today is “fast fashion” which has only recently gained significant traction and research focus.<sup>6,7</sup> This term derived from the quick-response (QR) business methodology in the 1980s, took off in the late 1990s, and has since been used in over six thousand publications cataloged within the Web of Science (WoS) to date.<sup>6,8–10</sup> Most typically, scientific studies focus on the impact of the textile industry on climate change and have provided strong evidence that recycling and reuse reduce environmental impact when compared to landfills

and incineration.<sup>11</sup> When we couple the terms “recycle” and “reuse,” then we are presented with a 2-fold increase in the number of publications; however, as observed by Sandin *et al.*, there exists scenarios where recycling and reusing are not the best solution and further studies must be performed for “end-of-life” treatment systems.<sup>11</sup> Herein, we present a method to not only recycle textiles but provide an end-of-life solution for several materials or material mixtures that would otherwise be incinerated.

Fast-fashion describes the rapid clothing supply chain where clothing suppliers respond to fashion trends within three to five weeks.<sup>6,8,9,12</sup> Typically, such a quick turnaround results in a shorter lifetime for the clothing.<sup>12–14</sup> Thus, presently, the production of fabric (fiber production, dyeing, incineration, *etc.*) comprises about 10% of global greenhouse gasses (GHG) emissions.<sup>2,15</sup> This means that 1.2 billion tons of GHG are emitted annually to produce and discard clothing.<sup>2,10,15,16</sup> Most clothing is discarded into a landfill as there exists no clearly established recycling method and furthermore, unsold clothing is often incinerated to maintain brand value.<sup>17,18</sup>

Fortunately, a new market has emerged where clothing can be resold or upcycled as done by such companies providing resources as ThredUp and Earth 911.<sup>19,20</sup> More importantly, companies such as ForDays and ReTold provide a user-friendly

<sup>a</sup>Department of Chemical and Biomolecular Engineering, University of Notre Dame, Notre Dame, IN 46530, USA. E-mail: nmyung@nd.edu

<sup>b</sup>Research Institute for Green Energy Convergence Technology (RIGET), Gyeongsang National University, Jinju 52828, Republic of Korea

† Electronic supplementary information (ESI) available: Additional pink sweater results; XRD peak deconvolution fitting example; XRD peak results; FTIR peak results; cantilever result fits and statistics. See DOI: <https://doi.org/10.1039/d2su00068g>



way to recycle textiles. For example, ReTold claims to have diverted 12 tons of textiles from landfills by providing purchasers a prepaid postage bag for easy drop-off.

There exists three major types of textile recycling: mechanical, chemical, or thermal (incineration that would preferably be avoided).<sup>11,21</sup> Textile recycle companies, like those mentioned above, rely heavily upon mechanical recycling methods whereupon textiles are sorted, cut, shred, mixed with virgin material, and re-spun into yarn to make new textiles or ground and pelletized, depending on the material type.<sup>22–25</sup> Mechanical recycling makes up the majority of the textile recycle methods available to consumers largely as a function of industrial ease as well as a function of the most commonly recycled fiber type (cotton).<sup>11,22,24</sup> As mentioned earlier, there exist few end of life resources or options for textiles; thus, to avoid incineration that would directly contribute to GHG emissions, we propose an alternative waste handling process for specific materials before or at the textiles' end of life *via* chemical separation, electrospinning synthetic techniques, and piezoelectric energy harvesting. By chemically digesting textile waste that can no longer be reused or recycled in the traditional sense, we can create nanofibrous materials with additional properties and uses. Arguably the amount of textile waste greatly outweighs the needed amount of material for energy harvesting devices, at least in the long run; however, this process is best suited for end-of-life treatment and not those materials that could otherwise be reused. Additionally, this process is most applicable to organic man-made materials, specifically those that are piezoelectric active. A hypothetical life cycle for a sustainable clothing system is illustrated in Fig. 1.

Generally speaking, research on energy harvesting from nanofibers is a well-established field with polymers such as polyvinylidene fluoride (PVDF), polyacrylonitrile (PAN), nylon, and poly(lactic acid) (PLLA) being used for such applications as triboelectric nanogenerators, diagnostic biocompatible sensors, face mask filters, and self-powering electrical stimulators, to name a few.<sup>26–33</sup> More specifically, PAN is a relatively

easily electrospun nanofiber material with recent publications citing a piezoelectric constant,  $d_{33}$ , value up to  $39 \text{ pm V}^{-1}$  through the control of the nanofiber diameter and confinement effect.<sup>34</sup>

In a recently published review article, we further detail flexible electrospun polymers and methods with which they can be optimized through factors including fine tuning of solutions, electrospinning environmental controls, post thermal treatments, and nanofiber properties such as resulting dimensions and morphology. Using design of experiments (DOE), any number of parameters can be tuned towards an enhancement of the piezoelectric phase and resulting piezoelectric output.<sup>35</sup> For example, by fine tuning of the electrospinning solution composition polymer and additive weight percents, Peidavosi *et al.* were able to increase the voltage output by 80%, up to 1.9 V, from a piezo-electrical stimuli scaffold designed for tissue engineering applications.<sup>36</sup>

PAN-based textiles where the copolymer contains a minimum of 85% acrylonitrile units are labeled as “acrylic” in our daily lives.<sup>37,38</sup> Acrylic fibers are typically used in clothing that form as knit textiles such as a scarf or hat; however, since these are products that are easily discarded after the winter season, a large amount of waste is generated. Another commonly discarded material is nylon as it is widely used for garments such as windbreakers, stockings, bags, belts, and coat linings.

Both of these short-lived textiles are composed of polymers known to be piezoelectric, where physical stress generates an electrical charge and where waste movement such as walking or tapping a finger could be harvested to power small electronic devices. For example, piezoelectric PAN has been used in an integrated nanofiber membrane for tiny-force sensing, real-time delamination failure monitoring, and nanogenerators.<sup>39–41</sup> Piezoelectric nylon has also been used in electronic textiles, battery separators, and a wearable Morse code detector.<sup>42–44</sup> Such devices can detect small perturbations making them ideal

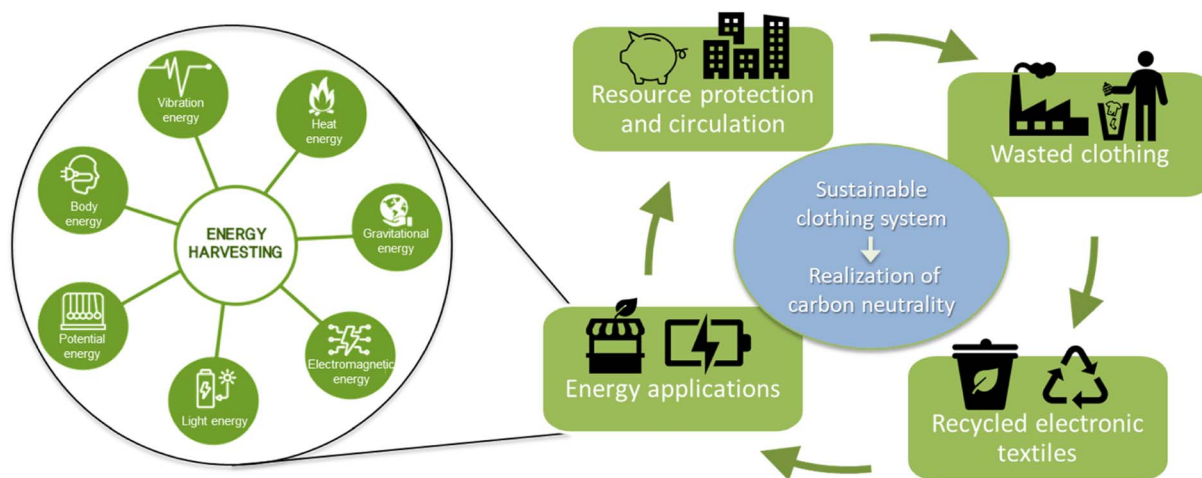


Fig. 1 A schematic illustrating the potential life cycle of textiles. Specific materials may contain piezoelectric components that upon separation could be used for energy harvesting or sensing applications.



for nano-type devices or biological applications that have become ubiquitous in everyday life.

During the process of electrospinning, the solvent evaporates, which could in turn be detrimental to the environment on a large scale. Recent publications have performed a life-cycle assessment of CO<sub>2</sub> capture from flue gasses from coal power plants where traditional methods could be modified and retrofitted for volatile organics capture.<sup>45,46</sup> Keeping this in mind, we propose that future work could aim to capture and recondense the highly volatile solvents that are evaporated during the electrospinning process thus making it a more environmentally friendly process and sustainable material cycle.

From clothing bought secondhand, we will demonstrate a scalable process that converts the used materials into a power generating electronic textile as illustrated in the Fig. 2 schematic. All secondhand clothing can be used as-is with no further purification needed; however, it should be noted that due to the nature of the material being used there exists impurities such as dyes and additional polymers that, while still soluble within this process, will not contribute to the piezoelectric response of the produced textile.

## Experimental

### Materials

Secondhand garments [acrylic sweaters (blue and pink) and nylon beige raincoat] were purchased from Goodwill. Polyacrylonitrile (PAN,  $M_w = 150\,000\text{ g mol}^{-1}$ ), nylon-6 (CAS-No. 25038-54-4, Product 181110) were purchased from Sigma Aldrich. *N,N*-dimethylformamide (DMF) and formic acid 98% were purchased from Fisher Scientific. All materials were used without further treatment or purification.

### Electrospinning

**Solution preparation.** The required amount of waste materials was weighed out to produce 11 wt% solutions. The acrylic sweaters and nylon raincoat were soaked in DMF or formic acid (98%), respectively, and then stirred at room temperature until homogeneous. Acrylic solutions were made under the assumption that the material was 100% PAN homopolymer, regardless of actual textile composition.

**Solution characterization.** Solution viscosity was measured using a Brookfield DV2THB viscometer and electrical

conductivity using a glass-body electrical conductivity probe ( $K = 1.0$ , Apera Instruments) paired with an embedded conductivity circuit (Atlas Scientific, EZO-ECTM) and an Arduino Uno Rev3 board. All solution properties measurements were taken at room temperature immediately before electrospinning to correlate them most closely to resulting nanofiber properties.

**Electrospinning.** The prepared PAN, nylon, recycled acrylic and recycled nylon solutions were drawn into a 5 mL BD Luer Lok syringe with a 25 or 20-gauge needle, which was then loaded onto a syringe pump (New Era, NE100). The needle tip was set at 10 cm from the drum collector. Negatively charged 16.5 and 21 kV were applied to the needle tip for PAN and acrylic solutions, respectively. The grounded drum collector was wrapped tightly with aluminum foil and rotating at 400 rpm. Environmental conditions were kept constant at temperature of 23 °C and absolute humidity of 0.005 kg water/kg dry air.

To demonstrate scalability, a needleless roll to roll electrospinning equipment (*i.e.*, Elmarco Nanospider NS lab system) was used to create large bolts of piezoelectric fabric. The prepared recycled acrylic and nylon solutions were poured into a 40 mL solution carriage with 0.7 mm orifice depending upon the viscosity of the solution. The carriage moved across the system, evenly coating the wire with the solution. The wire was negatively charged at 36–40 kV. The substrate above the moving carriage and wire is grounded and collects the nanofibers. The speed of the carriage, distance from the wire to the collector as well as the substrate moving speed can be varied depending upon the solution properties.

### Piezoelectric characterization

Two electrodes were made for each nanofiber sample to measure the voltage vertical to the direction of fiber length (denoted as  $V_{33}$ ). A  $7.2 \times 1.6 \times 0.01\text{ cm}^3$  brass substrate covered on both sides with polyimide tape was prepared as the cantilever. Nanofiber sample was fixed to the center of the cantilever with double-sided copper tape, which served as the bottom-contact electrode, while the other side of the nanofiber was insulated with polyimide tape. A pair of 24-gauge wires were soldered to the contact, sealed with polyimide tape, then connected to a breadboard with inputs to a Picoscope 2204 A™ (Pico Technology Ltd) to measure the absolute output voltage from the nanofiber mats.

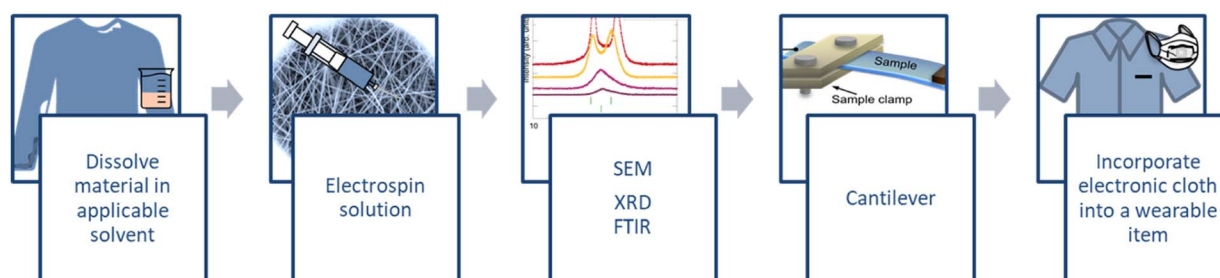


Fig. 2 A schematic illustrating the proposed end-of-life process for repurposing piezoelectric materials including synthesis, characterization, and possible outcome.





## Composition and structural characterization

Morphologies of the as-spun nanofiber and the composite materials were observed with a scanning electron microscope (SEM, ThermoScientific Prisma E). Prior to analysis, a thin layer of gold was sputtered over the samples at 20 mA for 30 seconds to minimize surface charging. Obtained SEM images were imported to ImageJ software to measure the average fiber diameter, which was obtained by measuring the length of 50–60 unique nanofibers. Bead density was calculated by dividing the total number of beads from a single SEM image by the total area of the image. Fiber fraction was determined by the proportion of nanofibers in the total product, which could include beads and clumps.

The molecular and crystal structures were observed throughout experiments with a Bruker Tenor 27 FTIR-ATR spectrometer and a Rigaku MiniFlex X-ray diffractometer, respectively. Fixed-angle FTIR-ATR was run from 4500–400  $\text{cm}^{-1}$  over 128 scans with a resolution of 4  $\text{cm}^{-1}$ . XRD was performed at room temperature with Cu-source from 10–45° in scattering angle ( $2\theta$ ) with 0.02° increment size.

## Results and discussion

Most garments are a blend of textiles, making recycling complicated as the separation is labor and energy intensive, often requiring a combination of mechanical, chemical, and thermal processes. This, compounded with the knowledge that materials labeled acrylic are copolymers with a minimum 85% acrylonitrile rather than homopolymers, it is expected that the generated voltage from an electrospun recycled material will not be of the same magnitude as that generated by a purchased, virgin chemical. While this expectation was met, as seen in Fig. 4, it was the simplicity in which a garment at the end of its life could be reformed into an energy generating electronic textile that drives the novelty of this work. The presence of polyacrylonitrile was confirmed within the waste sweater and recycled materials using  $^1\text{H-NMR}$ , as seen in ESI Fig. 6.†

Well worn, out-of-style garments (a sweater, raincoat, and child's sweater) were purchased at a secondhand store. The blue acrylic sweater and nylon raincoat were the primary materials analyzed and the pink acrylic sweater analysis is included in the ESI† as a proof of reproducibility. These garments, Fig. 3(a), were dissolved in a solution without further purification and then electrospun in both a multinozzle and needleless electrospinning configuration as detailed in the Experimental section. Just a small portion of the garments were needed to create a large bolt of nanofiber cloth as seen in Fig. 3(b) and ESI Fig. 1.† SEM images of the as-purchased waste materials and multinozzle electrospun nanofibers are shown in Fig. 3(a) and (b), respectively. Both materials display a marked decrease in fiber diameter upon transforming from woven to electrospun textile, from 18 to 25  $\mu\text{m}$  and 280 to 110 nm for acrylic and nylon, respectively. Once a fiber fraction, the fraction of fibers to total area, was confirmed greater than 95%, a small portion of the nanofiber mat was assembled in a cantilever device and the output voltage was analyzed at various levels of induced strain, as shown in Fig. 4. Dissolved and drop-cast materials were also tested for comparison.

The electrospun waste materials produced output voltages up to 550 mV. While that value is not particularly impressive, it should be noted that the results in Fig. 4(a) are a function of induced strain and directly depend upon other parameters such as sample thickness, fiber diameter, annealing temperature, *etc.* More concisely, these materials have yet to be optimized towards the highest voltage output. Furthermore, these materials were directly dissolved clothing with no purification and thus contain additives such as dyes that may inhibit the formation of the piezoelectric active phase during electrospinning. The waste materials, [a(top)] and [b(top)], had only 100 mV output which is within the background noise levels created by ambient vibrations and potential static interactions. Similarly, the drop cast film versions of each material had a voltage output of 150 mV or less. The electrospun versions of each material has a 4- to 5-fold increase, up to 550 mV for the

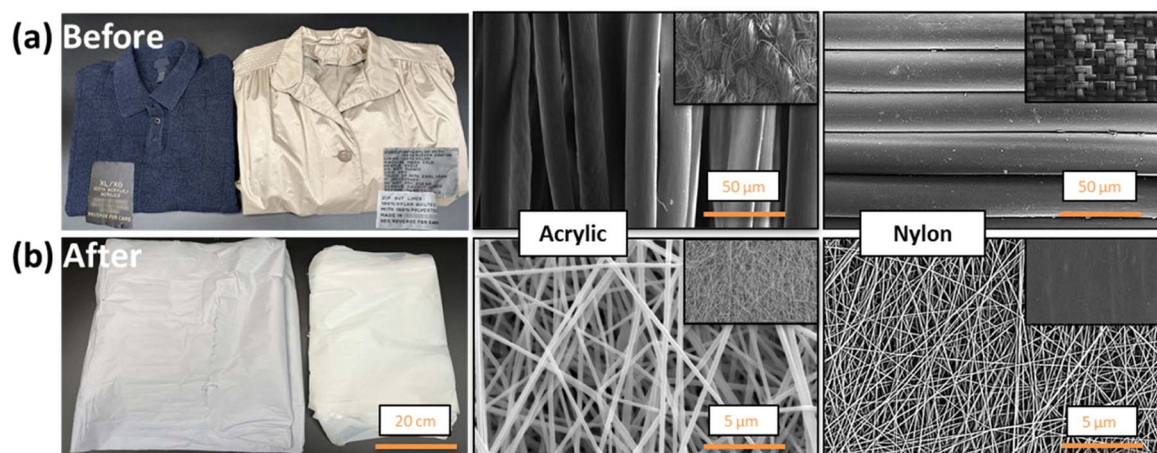


Fig. 3 A secondhand sweater and raincoat (a) before and (b) after dissolution and electrospinning to create electronic textiles. The blue sweater was acrylic, and the tan raincoat liner was nylon.



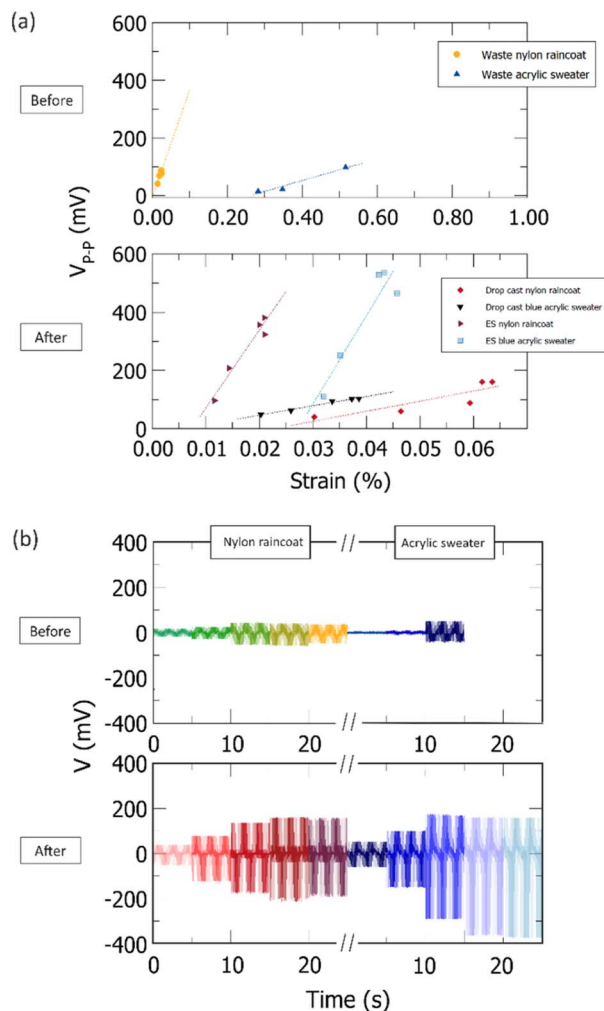


Fig. 4 Each second-hand textile, before (top) and after (bottom) processing and electrospinning, was studied using a cantilever device. (a) The output voltage as a function of strain for each comparable material was linearly fit. (b) The raw output voltage at various strain intensities, where green to yellow and red curves are the nylon material and blue curves are acrylic materials.

acrylic material and 350 mV for the waste nylon. This transformation to an electronic textile presents promising results given that experiments were performed with an 11 wt% unoptimized solution. Additionally, the waste materials could be further purified by chemical separation to remove dyes or other additives prior to use to further enhance performance.

Arguably, a more easily analyzed piezoelectric parameter is the linear fit of the output voltage as a function of strain. The slope, as listed in bold in ESI Table 3,<sup>†</sup> of the linearly fit line represents the sensitivity of each analyzed material. Using the obtained values, or from visual inspection, it can be seen that acrylic materials produce a higher piezoelectric response than nylon as well as requiring a higher degree of strain. This is expected given that polyacrylonitrile has a larger piezoelectric constant *versus* that of nylon.<sup>26,47</sup> It should be noted that the % strain of the waste materials was an order magnitude higher than the materials after electrospinning. This is attributed to

the relative thickness of each sample where strain is directly proportional to sample thickness based upon the cantilever beam equation. In Fig. 4(b), the waste acrylic sweater, prior to any processing, could at most be probed to 0.05% whereupon the sample began colliding with the sample base and nullifying any measurements.

To confirm and understand any structural or physical changes the samples underwent, XRD and FTIR were measured on the waste garments and compared to both the electrospun and drop cast materials [Fig. 5(a–d), respectively]. For the acrylic material, from the XRD data, a shift of the (100) peak at approximately  $17.5^\circ$  can be seen to lower  $2\theta$  which indicates an expansion of the unit cell and  $d$ -spacing as well as a substantial decrease in intensity. Typically, the piezoelectric active phase within PAN has a smaller unit cell and thus a shift to higher  $2\theta$  would be expected; however, there are two events occurring simultaneously that impact the chain packing. First, the drop cast and waste acrylic exhibit a smaller unit cell; however, this is to be expected for a material that can pack more tightly within a liquid. Thus, when the acrylic is electrospun, the unit cell expands as it becomes slightly more ordered, due to alignment of the monomers from the high electric field, as compared to the randomized packing of monomers in a film or drawn yarn.<sup>22,48</sup> Second, the decrease in intensity can be attributed to a decrease in the amount of sample present as the electrospun mat is porous. While the intensity decreases substantially from the drop cast and waste material, as compared to the ES (electrospun) material, there exists the emergence of a piezoelectric active peak at lower  $2\theta$  and therefore from the XRD, it is concluded that the acrylic material becomes more aligned and more piezoelectric active.

For nylon-6, the piezoelectric inactive phase is referred to as the  $\alpha$ -phase with two prominent peaks at  $21$  and  $24^\circ$  that correspond to the (200) and (010) reflections, respectively. The desired piezoelectric  $\gamma$ -phase has one predominant peak at  $22^\circ$  for the (001) reflection. It is therefore relatively easy to qualitatively discern the conversion of the nylon material from one phase to another. From the XRD data, it can be seen that both the waste raincoat and drop cast raincoat have predominantly ( $\approx 90\%$ )  $\alpha$ -phase with the acknowledgement that there exists a small amount of  $\gamma$ -phase present despite the synthetic method, as determined by peak deconvolution [ESI Fig. 3 and ESI Table 1<sup>†</sup>]. The act of electrospinning converts 50–70% of the material to the piezoelectric active  $\gamma$ -phase, as confirmed upon peak analysis. The waste raincoat and drop cast raincoat have a relatively consistent phase composition between the two samples, with a slight difference in the unit cell size as exemplified in the  $2\theta$  shift. The drop cast raincoat is shifted to slightly higher  $2\theta$  with sharper peaks indicating a smaller, more crystalline unit cell.

Analysis of FTIR data complemented the conclusions from the XRD analysis and additionally, for the acrylic samples, provided a more concrete quantification of the piezoelectric active phase present. For PAN, differences in the conformers are observed between  $1300$ – $1200\text{ cm}^{-1}$  where the peak at  $1250\text{ cm}^{-1}$  is correlated to the desired piezoelectric active zigzag conformer and the  $1230\text{ cm}^{-1}$  peak is correlated to the  $3^1$  piezoelectric



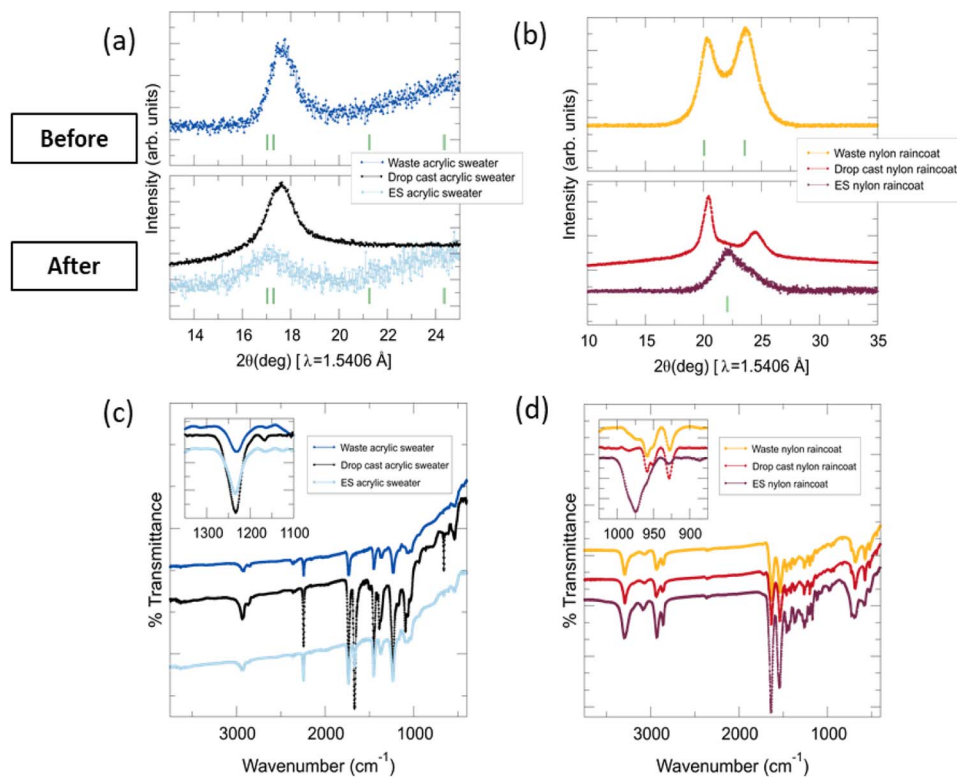


Fig. 5 XRD data of (a) acrylic and (b) nylon materials before (top) and after (bottom) processing. Observed sample data are indicated with data points and indexed crystallographic phases are green vertical tick marks. FTIR data of (c) acrylic and (d) nylon samples where each respective inset highlights the region at which peak deconvolution occurred to obtain sample composition.

inactive helical conformation. The proportion of area underneath the peaks at 1250 and 1230  $\text{cm}^{-1}$  relative to the total area underneath the peaks present from 1350 to 1100  $\text{cm}^{-1}$  is calculated to estimate the piezoelectric active content. Unsurprisingly, the waste sweater had 95% peak area present at 1232  $\text{cm}^{-1}$  and no peak present at 1250  $\text{cm}^{-1}$  indicating there exists no piezoelectric activity in this material. Upon electrospinning, a small peak at 1262  $\text{cm}^{-1}$  emerges with 7% relative peak area; yet almost 90% of the peak area remains at 1235  $\text{cm}^{-1}$ . This, combined with the decrease in peak intensity from the XRD data, leads to the conclusion that acrylic textiles can be recycled to electronic textiles but with a low, constant voltage output.

FTIR analysis of the nylon waste and newly created electronic material was performed by using the proportion of area underneath the peaks at 927 and 972  $\text{cm}^{-1}$  for the  $\alpha$ - and  $\gamma$ -phase, respectively, relative to the total area underneath the peaks present from 1050 to 875  $\text{cm}^{-1}$ . The waste raincoat had approximately equal parts of each phase in comparison to the XRD that concluded a predominantly  $\alpha$ -containing sample. However, upon electrospinning, the peak at 927  $\text{cm}^{-1}$  all but disappears which is consistent with XRD thus indicating a structural conversion of the waste raincoat to an electronic textile [see Fig. 5(b and d)]. Upon comparison of the drop cast nylon raincoat to the electrospun nylon raincoat, the difference in synthetic technique is highlighted. The drop cast nylon raincoat film exhibits several peaks within the analyzed range

however no peak around the expected 974  $\text{cm}^{-1}$  arises indicating little to no  $\gamma$ -phase is present. In contrast, the electrospun nylon raincoat has 51% of  $\gamma$ -phase that is a 2-times increase from the waste raincoat which is a direct result of the applied voltage from electrospinning.<sup>49,50</sup>

Ultimately, the XRD and FTIR data support the known phenomenon that electrospinning increases the piezoelectric active phase in piezoelectric capable polymers.<sup>51</sup> Both the waste acrylic sweater and nylon raincoat were dissolved and electrospun into piezoelectric active textiles.

For a further demonstration of the applicability of this end-of-life recycling process, the electrospun materials were analyzed as physical sensing (*e.g.*, strain sensor) devices within a cloth mask where facial movements, breathing, and speaking provided the mechanical perturbation for the piezoelectric device. A square piece of the recycled ES acrylic blue sweater was sandwiched between two conductive cloth pieces and care was taken to ensure that the cloth did not touch or that the nanofibers had torn, which would result in a system short. Leads were attached and connected to a microcontroller (*e.g.*, Adafruit QTPy) and other chemical sensors [*i.e.*, humidity, temperature, and total volatile organic compound (TVOC)], as shown in the block diagram in ESI Fig. 7.† The device and circuit boards were placed isolated within a sleeve in the cloth mask and worn for one minute. As seen in Fig. 6 and ESI Video clip,† the strain sensor made from ES blue acrylic sweater creates a detectable signal from breathing, speaking, and subsequent movement.





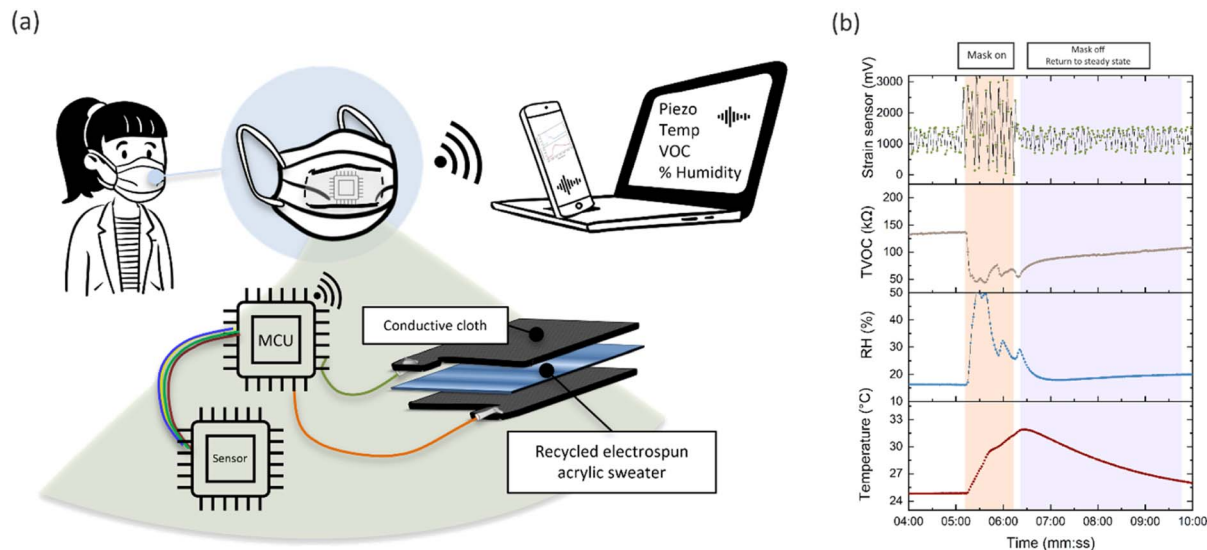


Fig. 6 (a) Conceptual schematic illustrating the potential application and implementation of recycled acrylic materials for piezoelectric sensing. (b) Raw data from a one-minute use of a cloth mask outfitted with the electronic textile made from recycled acrylic sweater and a Bosch BME680 sensor.

From Fig. 6(b), there exists a piezoelectric baseline between 800 and 1200 mV and the ES device more than doubles that response up to 3 V. During the one-minute interval, while being worn, the temperature unsurprisingly increases as well as the humidity. The chemiresistive gas sensor responds to total volatile organic compounds (TVOC) with a drop in resistance. In this case, the most abundant VOC is CO<sub>2</sub> expelled by the wearer. Several large breaths can be identified; however, higher sampling rates as well as faster recovery within the sensor itself would be required to distinguish unique breaths. Most interestingly, the ES recycled sweater had, at its highest, a 500 mV output when probed *via* the cantilever but within a more flexible sandwich (brass *vs.* cloth respectively), the material could output as high as 3 V.

## Conclusions

To create a more sustainable textile industry, we propose an alternative recycling route for select compositions towards energy harvesting applications through electrospinning. By modifying the substrate to a biologically friendly material such as polypropylene or polydimethylsiloxane, these materials could easily be comfortably placed or adhered to the skin. This demonstrates a full-cycle, alternative end-of-life treatment for specific textiles within fashion waste. Furthermore, this work demonstrates feasibility, ease, and a low-cost source for, at the minimum, preliminary scientific research involving electrospinning.

## Conflicts of interest

There are no conflicts to declare.

## Acknowledgements

This work was supported by the National Science Foundation (NSF CBET # 2040464). D. J. gratefully acknowledges support from NRF 202105610001.

## Notes and references

- M. Salvia, D. Reckien, F. Pietrapertosa, P. Eckersley, N. A. Spyridaki, A. Krook-Riekkola, *et al.*, Will climate mitigation ambitions lead to carbon neutrality? An analysis of the local-level plans of 327 cities in the EU, *Renewable Sustainable Energy Rev.*, 2021, **135**, 110253.
- L. Virta and R. Räisänen, Three Futures Scenarios of Policy Instruments for Sustainable Textile Production and Consumption as Portrayed in the Finnish News Media, *Sustainability*, 2021, **13**(2), 594.
- J. Payet, Assessment of Carbon Footprint for the Textile Sector in France, *Sustainability*, 2021, **13**(5), 2422.
- M. D. Stanescu, State of the art of post-consumer textile waste upcycling to reach the zero waste milestone, *Environ. Sci. Pollut. Res.*, 2021, **28**(12), 14253–14270.
- K. Riahi, C. Bertram, D. Huppmann, J. Rogelj, V. Bosetti, A. M. Cabardos, *et al.*, Cost and attainability of meeting stringent climate targets without overshoot, *Nat. Clim. Change*, 2021, **11**(12), 1063–1069.
- E. O. O. Rotimi, C. Toppo and J. Hopkins, Towards A Conceptual Framework of Sustainable Practices of Post-consumer Textile Waste at Garment End of Lifecycle: A Systematic Literature Review Approach, *Sustainability*, 2021, **13**(5), 2965.
- L. Claudio, Waste Couture: Environmental Impact of the Clothing Industry, *Environ. Health Perspect.*, 2007, **115**(9),



- A449–A454, available from: <https://ehp.niehs.nih.gov/doi/10.1289/ehp.115-a449>.
- 8 *Fashion Marketing: Contemporary Issues*, ed. T. Hines and M. Bruce, Routledge, 2012, available from: <https://www.taylorfrancis.com/books/9781136004261>.
  - 9 B. Lowson, R. King and A. Hunter, *Quick Response: Managing the Supply Chain to Meet Consumer Demand*, Wiley, Chichester, West Sussex, England ; New York, 1999, p. 281.
  - 10 A. Fotostock, The price of fast fashion, *Nat. Clim. Change*, 2018, **8**, 1.
  - 11 G. Sandin and G. M. Peters, Environmental impact of textile reuse and recycling – a review, *J. Cleaner Prod.*, 2018 May, **184**, 353–365.
  - 12 B. Zamani, G. Sandin and G. M. Peters, Life cycle assessment of clothing libraries: can collaborative consumption reduce the environmental impact of fast fashion?, *J. Cleaner Prod.*, 2017, **162**, 1368–1375.
  - 13 N. Le, *The Impact of Fast Fashion on the Environment*, Princeton Student Climate Initiative, 2020, available from: <https://psci.princeton.edu/tips/2020/7/20/the-impact-of-fast-fashion-on-the-environment>.
  - 14 T. Schlossberg, *How Fast Fashion Is Destroying the Planet*, The New York Times, 2019.
  - 15 T. Semba, Y. Sakai, M. Ishikawa and A. Inaba, Greenhouse Gas Emission Reductions by Reusing and Recycling Used Clothing in Japan, *Sustainability*, 2020, **12**(19), 8214.
  - 16 G. Qing, Y. Luo, W. Huang, W. Wang, Z. Yue, J. Wang, *et al.*, Driving Factors of Energy Consumption in the Developed Regions of Developing Countries: A Case of Zhejiang Province, China, *Atmosphere*, 2021, **12**(9), 1196.
  - 17 D. Damayanti, L. A. Wulandari, A. Bagaskoro, A. Rianjanu and H. S. Wu, Possibility Routes for Textile Recycling Technology, *Polymers*, 2021, **13**(21), 3834.
  - 18 E. Cline, Where Does Discarded Clothing Go?, *The Atlantic*, Business, 2014.
  - 19 Patagonia's Common Threads Garment Recycling Program: A Detailed Analysis, Patagonia, 2006, available from: [https://www.patagonia.com/on/demandware.static/Sites-patagonia-us-Site/Library-Sites-PatagoniaShared/en\\_US/PDF-US/common\\_threads\\_whitepaper.pdf](https://www.patagonia.com/on/demandware.static/Sites-patagonia-us-Site/Library-Sites-PatagoniaShared/en_US/PDF-US/common_threads_whitepaper.pdf).
  - 20 A. DuFault, *Can "Upcycling" Give Haiti's Fashion Industry a Boost?*, The Guardian, 2014.
  - 21 D. Glew, L. C. Stringer, A. A. Acquaye and S. McQueen-Mason, How do end of life scenarios influence the environmental impact of product supply chains? comparing biomaterial and petrochemical products, *J. Cleaner Prod.*, 2012, **29**(30), 122–131.
  - 22 F. A. Esteve-Turrillas and M. de la Guardia, Environmental impact of Recover cotton in textile industry, *Resour., Conserv. Recycl.*, 2017, **116**, 107–115.
  - 23 S. Yasin, N. Behary, M. Curti and G. Rovero, Global Consumption of Flame Retardants and Related Environmental Concerns: A Study on Possible Mechanical Recycling of Flame Retardant Textiles, *Fibers*, 2016, **4**(4), 16.
  - 24 K. Ragaert, L. Delva and K. Van Geem, Mechanical and chemical recycling of solid plastic waste, *Waste Manag.*, 2017, **69**, 24–58.
  - 25 S. S. Muthu, Y. Li, J. Y. Hu and P. Y. Mok, Recyclability Potential Index (RPI): the concept and quantification of RPI for textile fibres, *Ecol. Indic.*, 2012, **18**, 58–62.
  - 26 S. K. Nataraj, K. S. Yang and T. M. Aminabhavi, Polyacrylonitrile-based nanofibers—a state-of-the-art review, *Prog. Polym. Sci.*, 2012, **37**(3), 487–513.
  - 27 P. Martins, A. C. Lopes and S. Lanceros-Mendez, Electroactive phases of poly(vinylidene fluoride): determination, processing and applications, *Prog. Polym. Sci.*, 2014, **39**(4), 683–706.
  - 28 F. A. He, M. J. Kim, S. M. Chen, Y. S. Wu, K. H. Lam, H. L. W. Chan, *et al.*, Tough and porous piezoelectric P(VDF-TrFE)/organosilicate composite membrane, *High Perform. Polym.*, 2017, **29**(2), 133–140.
  - 29 A. Jamil, N. Mufti, S. Maryam, A. Hidayat, A. Taufiq and Sunaryono, Fabrication of PAN/ZnO Nanofibers by Electrospinning as Piezoelectric Nanogenerator, *J. Phys.: Conf. Ser.*, 2018, **1093**, 012024.
  - 30 Y. Tai, S. Yang, S. Yu, A. Banerjee, N. V. Myung and J. Nam, Modulation of piezoelectric properties in electrospun PLLA nanofibers for application-specific self-powered stem cell culture platforms, *Nano Energy*, 2021, **89**, 106444.
  - 31 G. Zhao, B. Huang, J. Zhang, A. Wang, K. Ren and Z. L. Wang, Electrospun Poly(L-Lactic Acid) Nanofibers for Nanogenerator and Diagnostic Sensor Applications, *Macromol. Mater. Eng.*, 2017, **302**(5), 1600476.
  - 32 X. Pu, J. W. Zha, C. L. Zhao, S. B. Gong, J. F. Gao and R. K. Y. Li, Flexible PVDF/nylon-11 electrospun fibrous membranes with aligned ZnO nanowires as potential triboelectric nanogenerators, *Chem. Eng. J.*, 2020, **398**, 125526.
  - 33 R. Das, E. J. Curry, T. T. Le, G. Awale, Y. Liu, S. Li, *et al.*, Biodegradable nanofiber bone-tissue scaffold as remotely-controlled and self-powering electrical stimulator, *Nano Energy*, 2020, **76**, 105028.
  - 34 S. Yu, J. Milam-Guerrero, Y. Tai, S. Yang, Y. Y. Choi, J. Nam, *et al.*, Maximizing Polyacrylonitrile Nanofiber Piezoelectric Properties through the Optimization of Electrospinning and Post-thermal Treatment Processes, *ACS Appl. Polym. Mater.*, 2022, **4**(1), 635–644.
  - 35 S. Yu, Y. Tai, J. Milam-Guerrero, J. Nam and N. V. Myung, Electrospun organic piezoelectric nanofibers and their energy and bio applications, *Nano Energy*, 2022, **97**, 107174.
  - 36 N. Peidavosi, M. Azami, N. Beheshtizadeh and A. Ramazani Saadatabadi, Piezoelectric conductive electrospun nanocomposite PCL/polyaniline/barium titanate scaffold for tissue engineering applications, *Sci. Rep.*, 2022, **12**(1), 20828.
  - 37 A. C. Nuessle and B. B. Kine, Acrylic Resins in Textile Processing, *Ind. Eng. Chem.*, 1953, **45**(6), 1287–1293.
  - 38 L. Rebenfeld, *Fibers and Fibrous Materials*, in: *Textile Science and Technology*, Elsevier, 2002, pp. 199–232, available from: <https://linkinghub.elsevier.com/retrieve/pii/S0920408302800093>.
  - 39 W. Jiang, K. Hu, N. Lv and Z. Lyu, Single flexible nanofibers to achieve simultaneous construction of piezoelectric





- elements and nanoresistance networks for tiny force sensing, *Sens. Actuators, A*, 2021, **332**, 113203.
- 40 L. Yuan, W. Fan, X. Yang, S. Ge, C. Xia, S. Y. Foong, *et al.*, Piezoelectric PAN/BaTiO<sub>3</sub> nanofiber membranes sensor for structural health monitoring of real-time damage detection in composite, *Compos. Commun.*, 2021, **25**, 100680.
- 41 Y. Sun, Y. Liu, Y. Zheng, Z. Li, J. Fan, L. Wang, *et al.*, Enhanced Energy Harvesting Ability of ZnO/PAN Hybrid Piezoelectric Nanogenerators, *ACS Appl. Mater. Interfaces*, 2020, **12**(49), 54936–54945.
- 42 S. Anwar, M. Hassanpour Amiri, S. Jiang, M. M. Abolhasani, P. R. F. Rocha and K. Asadi, Piezoelectric Nylon-11 Fibers for Electronic Textiles, Energy Harvesting and Sensing, *Adv. Funct. Mater.*, 2021, **31**(4), 2004326.
- 43 N. D. K. Tu, J. Park, S. Na, K. M. Kim, T. H. Kwon, H. Ko, *et al.*, Co-solvent induced piezoelectric  $\gamma$ -phase nylon-11 separator for sodium metal battery, *Nano Energy*, 2020, **70**, 104501.
- 44 K. Eom, S. Na, J. K. Kim, H. Ko, J. Jin and S. J. Kang, Engineering crystal phase of nylon-11 films for ferroelectric device and piezoelectric sensor, *Nano Energy*, 2021, **88**, 106244.
- 45 N. S. Matin and W. P. Flanagan, Life cycle assessment of amine-based *versus* ammonia-based post combustion CO<sub>2</sub> capture in coal-fired power plants, *Int. J. Greenhouse Gas Control*, 2022, **113**, 103535.
- 46 M. R. Mahi, I. Mokbel, L. Negadi, J. Saab and J. Jose, Volatility of monoethanolamine and tetramethylethylene diamine in aqueous solution for CO<sub>2</sub> capture at different loading, *Int. J. Greenhouse Gas Control*, 2022, **114**, 103598.
- 47 M. Smith and S. Kar-Narayan, Piezoelectric polymers: theory, challenges and opportunities, *Int. Mater. Rev.*, 2022, **67**(1), 65–88.
- 48 S. Yoon, S. Kim, C. W. Cho and Y. S. Yun, The Preparation of Modified Industrial Waste Polyacrylonitrile for the Adsorptive Recovery of Pt(IV) from Acidic Solutions, *Materials*, 2016, **9**(12), 988.
- 49 N. T. Srinivasan and M. Santappa, Polymerization of acrylonitrile, *Makromol. Chem.*, 1958, **26**(1), 80–91.
- 50 M. Kopeć, P. Kryś, R. Yuan and K. Matyjaszewski, Aqueous RAFT Polymerization of Acrylonitrile, *Macromolecules*, 2016, **49**(16), 5877–5883.
- 51 *Energy Harvesting Properties of Electrospun Nanofibers*, ed. J. Fang and T. Lin, IOP Publishing, 2019, available from: <https://iopscience.iop.org/book/978-0-7503-2005-4>.

